The EMBO Journal (2012) 31, 2810–2823 | © 2012 European Molecular Biology Organization | All Rights Reserved 0261-4189/12
www.embojournal.org

THE EMBO JOURNAL

A transcriptional repressor co-regulatory network governing androgen response in prostate cancers

Kern Rei Chng[1,2], Cheng Wei Chang[1,2], Si Kee Tan[1,2], Chong Yang[1,2], Shu Zhen Hong[1], Noel Yan Wei Sng[1] and Edwin Cheung[1,2,3,4,*]

[1]Cancer Biology and Pharmacology, Genome Institute of Singapore, A*STAR (Agency for Science, Technology and Research), Singapore, [2]Graduate School for Integrative Sciences and Engineering, National University of Singapore, Singapore, [3]Department of Biochemistry, Yong Loo Lin School of Medicine, National University of Singapore, Singapore and [4]School of Biological Sciences, Nanyang Technological University, Singapore

Transcriptional corepressors are frequently aberrantly over-expressed in prostate cancers. However, their crosstalk with the Androgen receptor (AR), a key player in prostate cancer development, is unclear. Using ChIP-Seq, we generated extensive global binding maps of AR, ERG, and commonly over-expressed transcriptional corepressors including HDAC1, HDAC2, HDAC3, and EZH2 in prostate cancer cells. Surprisingly, our results revealed that ERG, HDACs, and EZH2 are directly involved in androgen-regulated transcription and wired into an AR centric transcriptional network via a spectrum of distal enhancers and/or proximal promoters. Moreover, we showed that similar to ERG, these corepressors function to mediate repression of AR-induced transcription including cytoskeletal genes that promote epithelial differentiation and inhibit metastasis. Specifically, we demonstrated that the direct suppression of Vinculin expression by ERG, EZH2, and HDACs leads to enhanced invasiveness of prostate cancer cells. Taken together, our results highlight a novel mechanism by which, ERG working together with oncogenic corepressors including HDACs and the polycomb protein, EZH2, could impede epithelial differentiation and contribute to prostate cancer progression, through directly modulating the transcriptional output of AR.

The EMBO Journal (2012) **31,** 2810–2823. doi:10.1038/emboj.2012.112; Published online 24 April 2012
Subject Categories: signal transduction; chromatin & transcription; molecular biology of disease
Keywords: androgen receptor; EZH2; HDAC; prostate cancer; TMPRSS2:ERG

Introduction

The androgen receptor (AR) occupies a central role in the biology of both normal prostate development and prostate cancer progression (Shen and Abate-Shen, 2010). AR is a member of the nuclear hormone receptor superfamily that directs the transcriptional regulation of genes governing a wide variety of cellular processes including cell cycle, cell proliferation, survival, and differentiation (Schiewer *et al*, 2012). Upon activation by androgens, AR dissociates from heat shock proteins, dimerizes, and translocates from the cytoplasm into the nucleus where it recognizes and binds to androgen response elements near target genes (Heinlein and Chang, 2004). In normal cells, the transcriptional activity of AR is delicately controlled by the coordinated recruitment of specific coregulatory proteins (i.e. coactivators, corepressors, collaborative factors, *etc*), however, these proteins become aberrantly expressed in prostate cancers resulting in a deregulated AR transcriptional network (Pienta and Bradley, 2006; Shen and Abate-Shen, 2010).

Collaborative factors of AR that have been reported to be frequently over-expressed in prostate cancers include FoxA1, GATA2 (Wang *et al*, 2007), and members of the ETS family (Tomlins *et al*, 2005). The ETS family has received much attention lately because recent studies by Chinnaiyan and colleagues revealed that the majority of prostate cancers harbor recurrent fusion transcripts between the promoter region of the AR direct target gene, TMPRSS2, with different ETS members, resulting in the androgen stimulated over-expression of ETS transcription factors (Tomlins *et al*, 2005; Kumar-Sinha *et al*, 2008). The most important and common ETS fusion transcription factor appears to be TMPRSS2:ERG, which is detected in approximately half of all localized prostate cancers (Kumar-Sinha *et al*, 2008). Intriguingly, in contrast to its counterparts ETS1 and ETV1 (Massie *et al*, 2007; Shin *et al*, 2009), ERG was shown to attenuate AR-dependent transcription (Sun *et al*, 2008; Yu *et al*, 2010b). This finding suggests that the induction of ERG by AR could possibly feedback to perturb and deregulate the transcriptional network of AR. The detailed mechanism of attenuation and functional consequences associated with AR and ERG transcriptional crosstalk are currently still unclear.

Transcriptional corepressors that are associated with malignancies such as histone deacetylases (HDACs) and histone methyltransferases (HMTs) are also commonly over-expressed in prostate cancers (Varambally *et al*, 2002; Weichert *et al*, 2008). HDACs are a class of enzymes that regulate the transcription of target genes by catalyzing the removal of acetyl groups from either transcription factors or the tails of histones (Glozak and Seto, 2007). HDAC1, HDAC2 and HDAC3 are frequently over-expressed and have been shown to promote metastasis in prostate cancers (Weichert *et al*, 2008; Wang *et al*, 2009). Interestingly, high levels of HDAC1 coupled with a low expression of its target genes appears to be key characteristics of TMPRSS2-ERG fusion positive prostate cancers (Iljin *et al*, 2006; Gupta *et al*, 2010). Furthermore, ERG fusion positive prostate cancer cells are exceptionally sensitive to HDAC inhibitors (Bjorkman

*Corresponding author. Cancer Biology and Pharmacology, Genome Institute of Singapore, 60 Biopolis Street, #02-01 Genome, Singapore 138672, Singapore. Tel.: +65 6808 8184; Fax: +65 6808 8305; E-mail: cheungcwe@gis.a-star.edu.sg

Received: 20 October 2011; accepted: 29 March 2012; published online: 24 April 2012

et al, 2008). Consequently, epigenetic reprogramming through HDAC1 was proposed as a possible mechanism by which ERG fusion positive prostate cancers drive oncogenicity (Bjorkman *et al*, 2008). The HMT, enhancer of zeste homolog 2 (EZH2), is a member of the polycomb group family that suppresses gene transcription by catalyzing the trimethylation of histone H3K27 at the promoter of target genes (Cao and Zhang, 2004). High levels of EZH2 are commonly found in invasive and hormone refractory prostate cancers (Varambally *et al*, 2002). Recent studies suggest EZH2 may promote prostate cancer progression and contribute to metastasis by repressing the expression of developmental regulators and tumor suppressors, as well as activating the cellular de-differentiation program responsible for maintaining prostate cancer cells in a stem cell-like state (Cao *et al*, 2008; Yu *et al*, 2007b, 2010a, 2010b). In addition, the epigenetic silencing of DAB2IP by EZH2 may also trigger prostate cancer metastasis via activation of the RAS and NFKB signalling pathways (Min *et al*, 2010).

The collaboration between AR, ERG, HDACs and EZH2 is of exceptional therapeutic interest as it represents a cancer specific transcription co-operation that does not exist under normal circumstances. Even though all of the factors are important in prostate cancer progression, their relationship with each other remains largely unknown. Herein, we investigated and characterized the transcriptional crosstalk between AR, ERG, the corepressor proteins HDAC1, HDAC2, HDAC3, and EZH2 in prostate cancer cells upon androgen signalling. Overall, our results revealed that ERG promotes prostate cancer progression by working together with HDACs and EZH2 to directly modulate the transcriptional output of AR.

Results

DHT stimulates differential expression and binding of AR and ERG at ARBS

TMPRSS2:ERG is regulated by androgen stimulation and is found over-expressed in a large proportion of prostate cancer tumors (Tomlins *et al*, 2005). Despite recent efforts to unravel the transcriptional crosstalk between AR and ERG, the underlying mechanism of how androgen signalling affects the genome-wide binding of these factors to chromatin in prostate cancer cells is unclear. To address this, we first examined the effect of dihydrotestosterone (DHT) on the mRNA and protein expression level of AR and ERG. As shown in Figure 1A and B, DHT repressed the level of AR mRNA across time, while the protein level remained relatively constant with only a slight decrease after long DHT exposure (Figure 1B). In contrast, DHT up-regulated both the mRNA and protein levels of ERG although with different kinetics (peaking at 12 h for RNA and 24 h for protein) (Figure 1A and B). We next examined the binding of AR and ERG to chromatin upon DHT stimulation. Because of the differential expression of these proteins in response to DHT, we performed AR and ERG ChIP at various times after DHT stimulation. As shown in Figure 1C, AR was recruited strongly to the enhancer AR binding site (ARBS) of PSA 2 h after DHT stimulation, however, the binding was reduced significantly after 18 h. In comparison, ERG was also recruited to the ARBS of PSA and to the previously identified ERG binding site (ERGBS) associated with PLA1A 2 h after DHT treatment. However, unlike AR, the recruitment of ERG

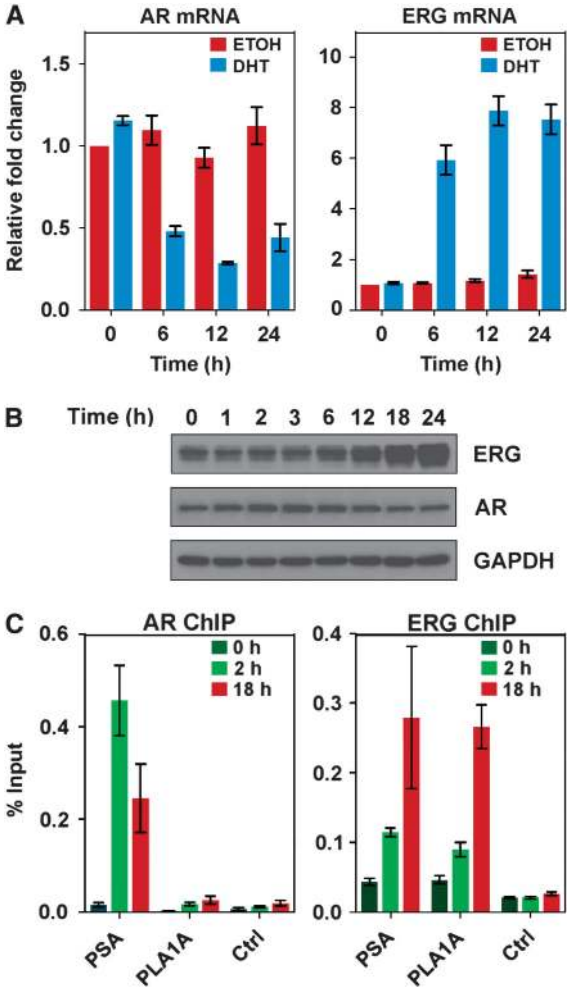

Figure 1 Androgen stimulates distinct expression and chromatin binding profiles for AR and ERG in prostate cancer cells. Time course expression analysis of AR and ERG (**A**) mRNA and (**B**) protein levels in VCaP cells after stimulation with 10 nM DHT at various time points. Error bars represent s.e.m. of at least 3 independent repeats. (**C**) Androgen stimulates AR and ERG binding to chromatin. Hormone depleted VCaP cells were treated with 100 nM DHT for 0, 2, or 18 h. Cells were cross-linked with formaldehyde and chromatin was immunoprecipitated with antibodies against AR or ERG. Immunoprecipitated DNA was quantified with qPCR for specific binding sites and a selected genomic location as control (ctrl) region. Error bars represent s.e.m. of at least 3 independent experiments.

was further enhanced after 18 h. Taken together, our results demonstrate that AR and ERG can be co-localized together upon androgen signalling, but the binding kinetics of the two transcription factors to chromatin are distinct.

Global analysis of AR and ERG binding sites

To expand our understanding of the temporal and spatial binding of AR and ERG in prostate cancer, we decided to perform ChIP-Seq of both factors in VCaP cells at 0, 2 and 18 h after DHT stimulation (Supplementary Table S1). Overall, we observed an increase in the number of AR and ERG (AR + ERG) co-localized binding events from 0 to 18 h, which was largely due to a sharp increase in AR binding after DHT stimulation (Figure 2A). *De novo* motif analysis of ARBS and ERGBS revealed the presence of canonical androgen response element (ARE) and ETS like motifs, respectively

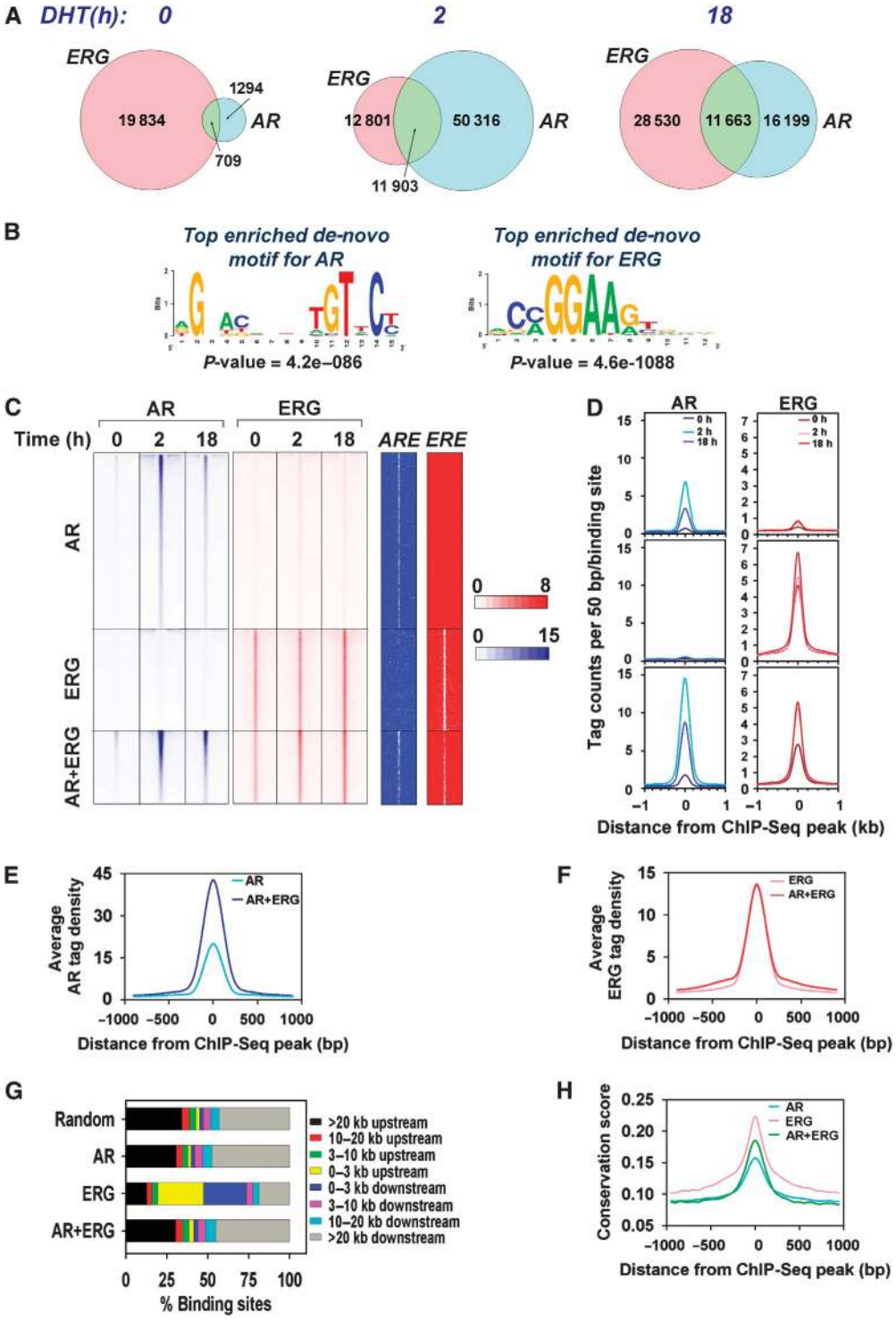

Figure 2 Global analysis of AR and ERG binding across the prostate cancer genome. (**A**) Venn diagram illustrating the overlap of AR and ERG cistromes in VCaP cells treated with 100 nM DHT at various time points (0, 2, 18 h). (**B**) Weblogo output of top enriched motif from AR (left) and ERG (right) ChIP-Seq peaks. A *de novo* motif discovery algorithm, MEME, was performed on the top 1000 ranked AR and ERG (DHT) ChIP-Seq peaks (± 50 bp from center of the ChIP-Seq peak). (**C**) Heatmap representation of sorted ChIP-Seq signals of AR and ERG binding events in VCaP cells. Signals are centralized to either the center of AR or ERG ChIP-Seq peak (± 2 kb). Corresponding occurrence of predicted ARE and ETS binding motif are depicted in heatmap on the right. (**D**) A comparison of the average AR and ERG ChIP-Seq tag intensities at different subsets of the AR and ERG cistrome after 0, 2, and 18 h of androgen stimulation. Comparison of the average binding intensities of (**E**) AR at AR binding sites with or without ERG occupancy, and (**F**) ERG at ERG binding sites with or without AR occupancy. (**G**) Global distribution of AR and ERG binding events with respect to the transcription start sites (TSSs) of RefSeq genes. (**H**) Conservation analysis of AR and ERG binding sites.

(Figure 2B). The global binding profiles of the two factors, as our results at individual locus already eluded (Figure 1C), were distinct for both factors upon DHT stimulation. In general, there was minimal AR binding in the genome prior to any stimuli (Figure 2C and D). AR binding at AR unique and AR + ERG co-localized sites occurred mostly after 2 h of

DHT stimulation. After 18 h of DHT treatment there was a global reduction in AR occupancy, an indication that at this phase of androgen signalling, the rate of AR recruitment may be outpaced by the rate of AR dissociation (Figure 2D). Surprisingly, in contrast to AR, there was a substantial amount of ERG occupancy at both ERG unique and AR + ERG co-localized binding sites prior to DHT stimulation (Figure 2C and D). The binding of ERG at AR + ERG co-localized binding sites was for the most part enhanced after 2 h DHT treatment, but not at ERG unique binding sites which suggests that at shared binding sites, AR could be enhancing ERG loading (Figure 2C and D). ERG binding at ERG unique sites eventually increased but only at the late phase of androgen signalling (18 h) (Figure 2C and D). This effect could possibly be due to a result of increased ERG protein expression. AR and ERG consensus motifs were found strongly enriched at AR + ERG overlap binding sites, which indicated that the presence of binding motifs is one of the major determinants of AR and ERG co-occupancy. Finally, we noticed that AR recruitment was overall significantly stronger (based on the average ChIP-Seq tag counts) at AR + ERG co-localized binding sites compared to AR unique sites (Figure 2E), whereas ERG recruitment was the same regardless whether it was at AR + ERG co-localized binding sites or at ERG unique sites (Figure 2F), suggesting that sites with stronger AR binding will favor ERG recruitment over their weaker counterparts.

We also examined the distribution of AR and ERG binding sites across the genome. Similar to previous observations (Wang *et al*, 2007), our AR ChIP-Seq showed ARBS are mostly located at regions that are far away from the transcriptional start sites (TSS) of genes (Figure 2G). In contrast, ERGBS can be found at both promoter and distal sites. As for AR and ERG co-localized binding sites, they were in general distributed far away from the TSS, similar to the overall positioning of ARBS (Figure 2G). In evolutionary conservation analysis, AR and ERG binding sites were generally more conserved at the region of the ChIP-Seq peak center relative to their flanking regions (background) (Figure 2H). ERG binding sites were the most conserved compared to AR unique and AR + ERG co-occupied binding sites (Figure 2H), probably as a result of ERGBS being localized to the generally well conserved TSS of genes. AR + ERG overlapping binding sites, possibly owing to their higher functional importance, were more conserved than AR unique binding sites (Figure 2H).

To examine whether AR unique and AR + ERG binding sites regulate similar or different androgen-mediated transcriptional programs, we performed an Ingenuity systems Pathway Analysis (IPA) for androgen-regulated genes associated with either AR unique or AR + ERG binding sites. As shown in Supplementary Table S2, AR + ERG binding sites were more associated with transcription programs related to cellular movement, cellular growth and proliferation, cell cycle and cell morphology, while AR unique binding sites were more associated with a transcription program linked to cell death. Taken together, our results indicate that AR and ERG binding across the genome is distinct yet share a large overlap, suggesting potential collaboration between these two factors.

Transcriptional collaboration between AR and ERG

The substantial overlap of the AR and ERG cistromes suggests that ERG may play a direct role in regulating AR-dependent transcription. Indeed, we noticed ERG co-localized with AR at a large number of well-known androgen-regulated genes including PSA (Figure 3A) and FKBP5 (Figure 3B). To determine if ERG is important for androgen-dependent transcription, we examined the effect of siRNA-mediated knockdown of ERG on AR target gene expression. As shown in Supplementary Figure S1, silencing of ERG affected both androgen up- and down-regulated genes. Interestingly, ERG knockdown enhanced the mRNA expression levels of a large set of androgen-upregulated genes (393) including PSA and FKBP5 (Figure 3C–E and Supplementary Figure S1), suggesting that one of the major roles of ERG is to attenuate the AR transcription response. We next examined the potential mechanism underlying ERG-mediated attenuation of androgen-dependent transcription by testing the possibility that ERG might be suppressing the recruitment of AR to chromatin. To do this, we performed AR ChIP after treating VCaP cells with or without siRNA directed against ERG. Silencing of ERG led to a significant increase in the binding of AR at numerous AR + ERG binding sites including those associated with PSA and FKBP5 (Figure 3F and G and Supplementary Figure S2) To determine the effect of ERG on global AR binding, we examined the AR ChIP-Seq dataset after ERG knockdown recently generated by Yu *et al* (2010b). As shown in Supplementary Figure S2, a large number of new ARBS appeared after ERG knockdown. Taken together, our results and that of Yu *et al* (2010b) suggest that the antagonistic effect of ERG on AR transcriptional activity could in part be attributed to the reduction of AR recruitment to its cis-regulatory elements by ERG.

Integrative transcriptional network between AR, ERG, and transcriptional corepressors in prostate cancer cells

Histone deacetylases, such as HDAC1, HDAC2, and HDAC3, and the methyltransferase, EZH2, are transcriptional corepressor proteins that are commonly found over-expressed in prostate cancers (Figure 4A) (Varambally *et al*, 2002; Weichert *et al*, 2008), positively correlated with ERG levels (Iljin *et al*, 2006; Yu *et al*, 2010b), and play important roles in the progression of the disease (Yu *et al*, 2007b, 2010a; Wang *et al*, 2009; Min *et al*, 2010). However, whether these corepressors are directly involved in regulating ERG-mediated inhibition of AR transcriptional activity has not been addressed. Previous studies have shown that HDACs can be recruited to ARBS, however this was in the context of AR-dependent transcriptional repression under antiandrogen (casodex) stimulation (Shang *et al*, 2002). Although no evidence to date indicates EZH2 is directly involved in AR-mediated transcription, it has however been shown to be important in regulating the activities of other transcription factors such as NFkB (Lee *et al*, 2011). Based on these findings, we asked whether the attenuation of AR transcriptional activity that we observed above could be due the recruitment of one or more of these corepressors to AR and ERG co-localized binding sites. To test this hypothesis, we performed ChIP assays for HDACs and EZH2 in VCaP cells before and after DHT treatment. Surprisingly, we found HDAC1, HDAC2, HDAC3, and EZH2 were all recruited to several AR and ERG co-localized binding sites including those associated with PSA and FKBP5 (Figure 4B). Furthermore, the recruitment of these corepressors was in most cases enhanced by DHT stimulation. To assess

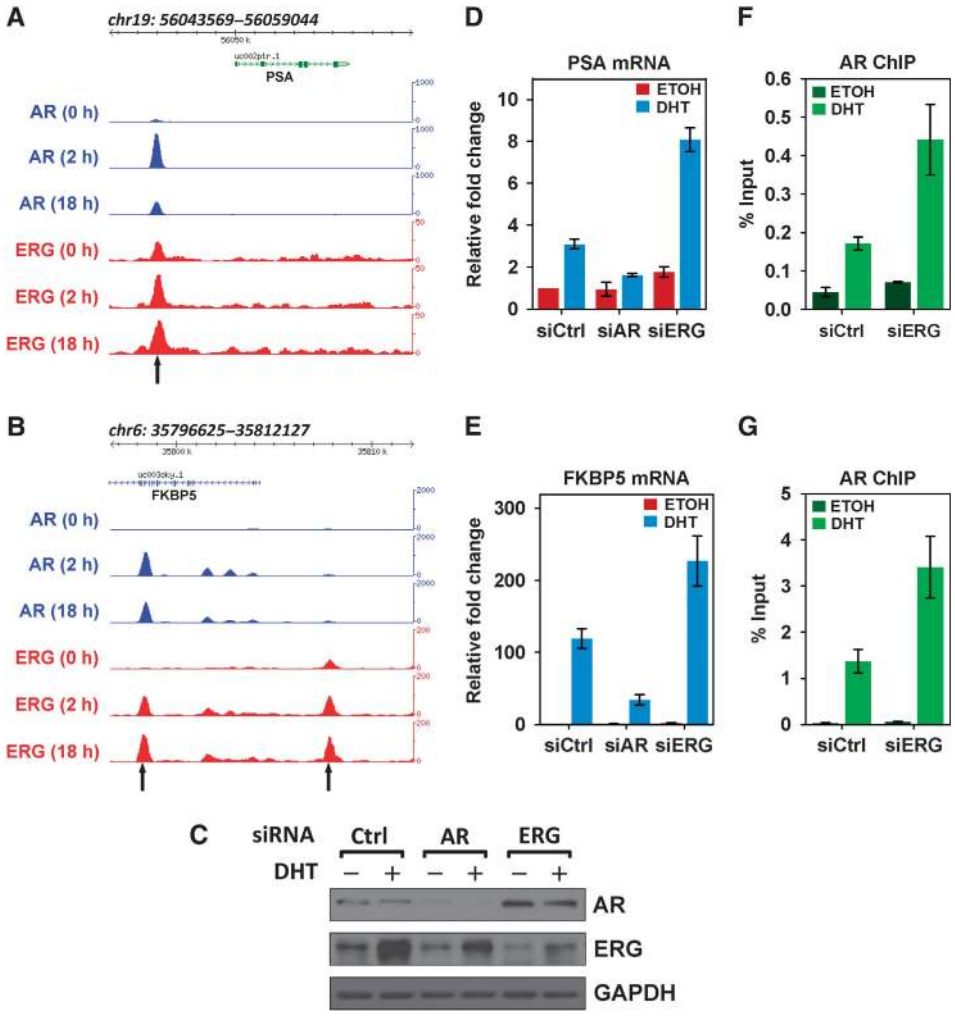

Figure 3 ERG attenuates androgen-dependent transcription by inhibiting AR binding. Snapshots showing the co-localization of AR and ERG binding sites at two model AR target genes: (**A**) PSA and (**B**) FKBP5. The black arrows indicate the co-localized AR and ERG binding sites examined. (**C**) Western blot analysis showing AR and ERG expression in androgen deprived VCaP cells treated with EtOH or 10 nM DHT for 18 h after being transfected with control siRNA or siRNA against AR or ERG. GAPDH was used as a loading control. (**D**) and (**E**) ERG regulates AR-dependent transcription. VCaP cells were transfected with control siRNA or siRNA targeting AR or ERG. After 8 h of EtOH or 10 nM DHT stimulation, cells were harvested for total RNA, converted to cDNA before quantifying gene expression levels. GAPDH was used as a control for internal normalization. Error bars represent s.e.m. of at least 3 independent experiments. (**F**) and (**G**) ERG inhibits AR binding. VCaP cells transfected with control siRNA or siRNA targeting ERG were deprived of androgens for 24 h before being stimulated with EtOH or 100 nM DHT for 2 h. ChIP assays with antibodies against AR were performed and immunoprecipitated DNA was quantified with qPCR for specific binding sites. Error bars represent s.e.m. of at least 3 independent experiments.

recruitment of these co-repressors to AR and ERG co-localized binding sites in further detail, we performed a time course ChIP of these factors after androgen stimulation. In general, HDAC1-3 and EZH2 were recruited to ARBS as early as 15 mins after androgen stimulation, with similar binding profile as AR (Supplementary Figure S3). Taken together, our results suggest that HDACs and EZH2 are recruited to AR and ERG co-localized sites and may co-operate with ERG in mediating the inhibition of androgen-dependent transcription.

To determine the extent of co-operation between AR, ERG and the corepressors, HDACs and EZH2, we performed ChIP-Seq of these factors in VCaP cells before and after 2 h of DHT stimulation, the time-point corresponding to the largest overlap in AR and ERG co-localized binding (Supplementary Table S3). We first examined the ChIP-Seq peaks of the corepressors for motif enrichment using CENTDIST (Zhang *et al*, 2011) and found good center of distribution scores for sequences representing both AR and ERG at HDAC2, HDAC3, and EZH2 binding sites, suggesting that these corepressors may be indirectly recruited to chromatin via AR and ERG (Figure 5A). In comparison, only ERG motifs were enriched for HDAC1, which indicate that HDAC1 is likely recruited mainly through ERG.

We also examined the genomic distribution of the corepressors with respect to known genes. In general, the cistrome of each individual corepressor exhibited distinct binding characteristics. For instance, HDAC1 appeared to be preferentially located at promoters, while HDAC2 and HDAC3 were predominantly found at distal enhancers (Figure 5B). From previous binding studies of EZH2, it was generally thought that EZH2 binds mainly to promoter regions (Yu *et al*, 2007a; Ku *et al*, 2008; Margueron *et al*, 2008), however from our genome-wide analysis it appears that a large

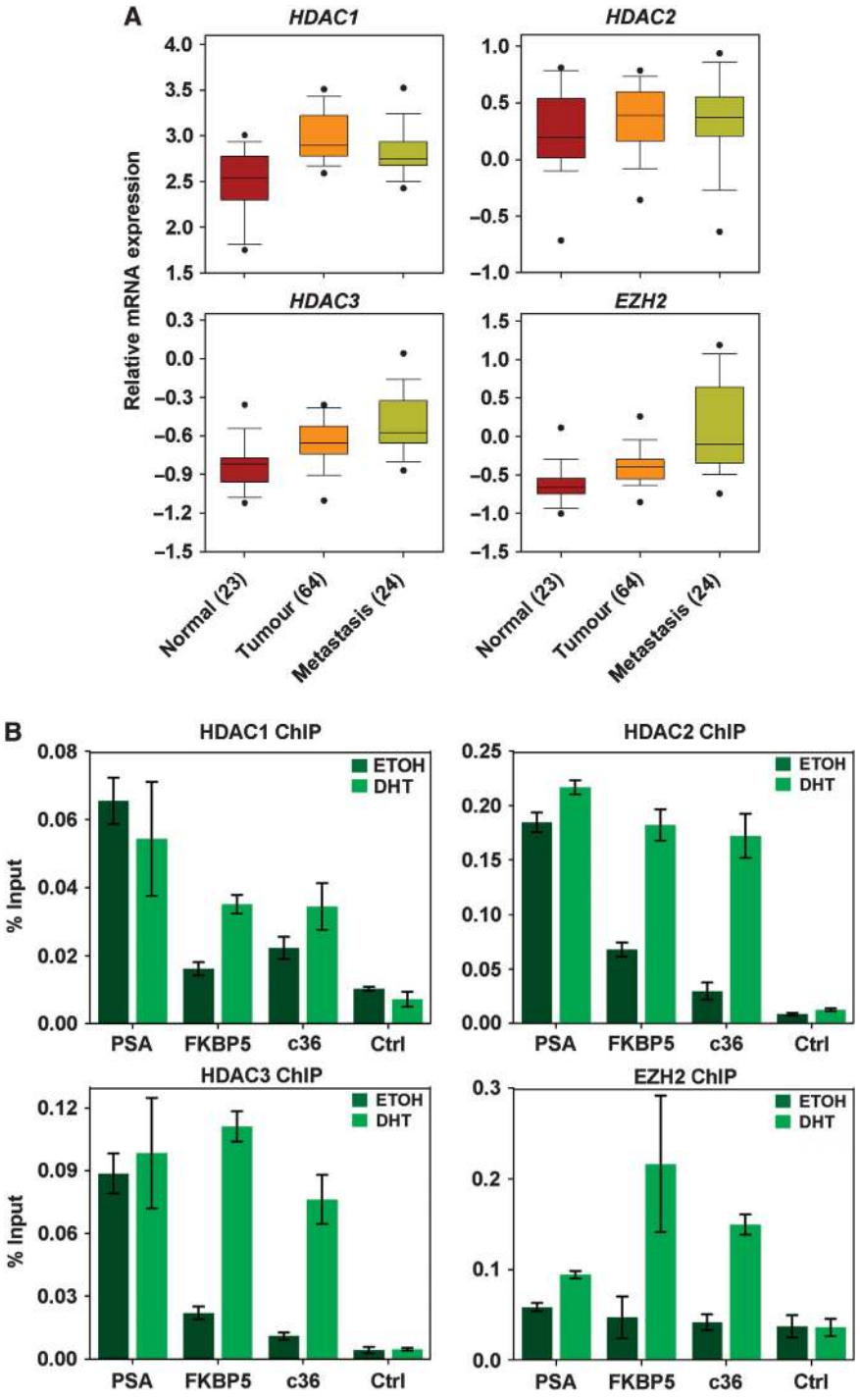

Figure 4 HDACs and EZH2 are recruited to AR binding sites. (**A**) Boxplots showing the relative mRNA expression levels of HDAC1, HDAC2, HDAC3, and EZH2 in clinical prostate samples from the Yu *et al* (2004) study, which has been deposited in the Oncomine database. (**B**) Androgen-depleted VCaP cells were treated with either EtOH or 100 nM DHT for 2 h. The cells were then double crosslinked with DSG followed by formaldehyde. Chromatin was immunoprecipitated with antibodies against HDAC1, HDAC2, HDAC3, or EZH2. Immunoprecipitated DNA was quantified with qPCR for specific binding sites and a selected genomic location as a control (ctrl) region. Error bars represent s.e.m. of at least 3 independent experiments.

proportion of EZH2 are actually found at distal enhancers after androgen stimulation (Figure 5B). With respect to AR and ERG binding, we also found distinct combinations of corepressor recruitment. AR and ERG co-localized sites recruited mainly HDAC2, HDAC3, and EZH2, whereas AR unique binding sites also recruited these same factors but to a much lesser degree (Figure 5C and D and Supplementary Figure S4). In contrast, HDAC1 and -2, but not EZH2 were recruited to ERG unique binding sites. We also noticed that HDAC2, HDAC3 and EZH2 occupancy at ARBS sites were enhanced upon androgen stimulation, with the strongest increment (average ChIP-Seq tag count) at AR and ERG

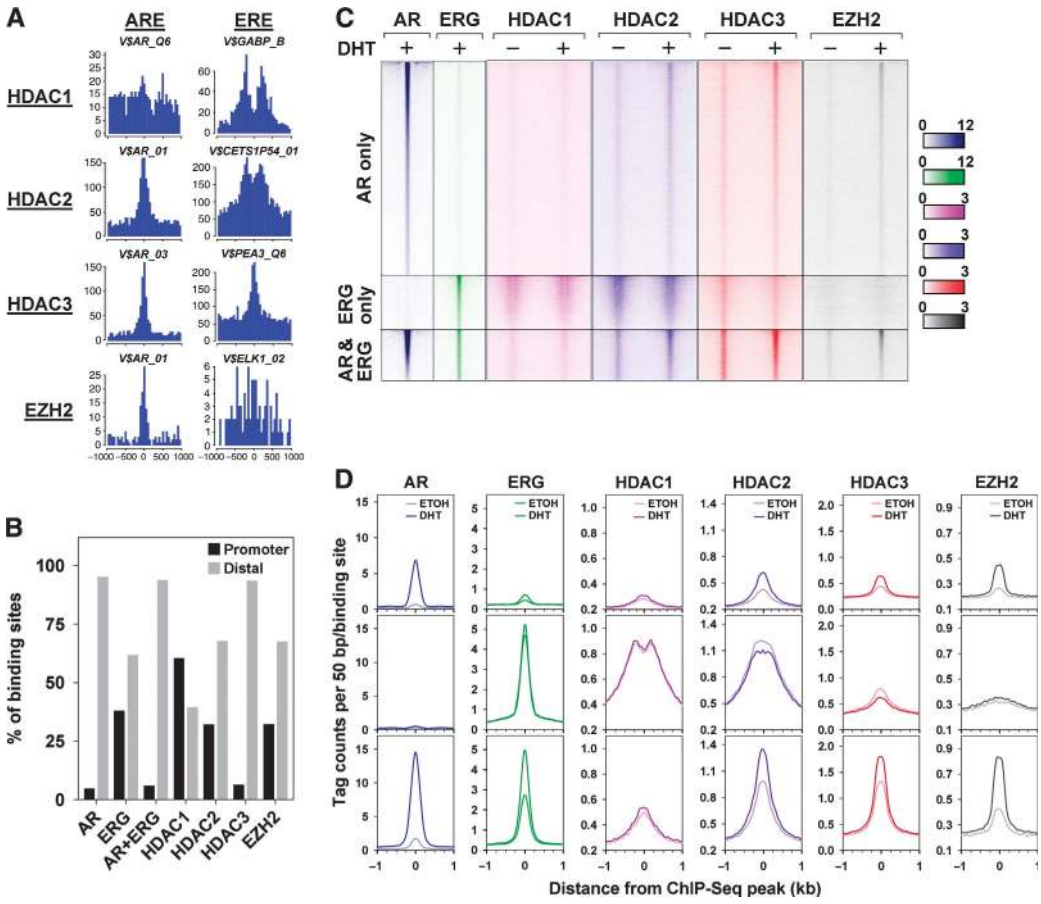

Figure 5 An integrated transcriptional network of AR, ERG, HDACs and EZH2 in prostate cancer. HDAC1, HDAC2, HDAC3 and EZH2 binding sites (under 2 h DHT stimulation) were examined using CentDist (Zhang *et al*, 2011). (**A**) Graphs showing the average distribution of Androgen Response Elements (AREs) and ETS response elements (EREs) centered at the peaks of the binding sites of the respective corepressor. (**B**) Bar chart showing the percentage binding sites located at the promoter proximal (±3 kb from TSS) and distal regions for AR, ERG, HDAC1, HDAC2, HDAC3, and EZH2. (**C**) Heatmap representation of sorted ChIP-Seq signals of AR, ERG, HDAC1, HDAC2, HDAC3, and EZH2 binding events in VCaP cells. Signals are centralized to either the center of AR or ERG ChIP-Seq peak (±2 kb). (**D**) A comparison of the average ChIP-Seq tag intensities of AR, ERG, HDAC1, HDAC2, HDAC3, and EZH2 at different subsets of the AR and ERG cistrome after 2 h of androgen stimulation.

co-occupied sites (Figure 5D). In comparison, no changes in HDAC1 binding were observed at the same binding sites (Figure 5D). Taken together, our ChIP-seq results show that HDACs and EZH2 are directly integrated in the androgen signalling network and regulate AR- and ERG-dependent transcription by occupying different subsets of the AR and ERG cistrome.

HDACs and EZH2 function together with ERG and AR to attenuate androgen-dependent transcription

The recruitment of HDACs and EZH2 to AR and ERG co-localized binding sites across the prostate cancer genome suggests these corepressors are involved in ERG-mediated inhibition of androgen-dependent transcription. Consistent with this, we found HDACs and EZH2 recruited to AR and ERG co-localized binding sites associated with androgen direct target genes including PSA and FKBP5 (Figure 6A). To determine whether HDACs and EZH2 are important in suppressing androgen-dependent transcription, we examined the transcript levels of PSA and FKBP5 after blocking the activities of the corepressors with specific small molecule inhibitors. Specifically, we used TSA and DZNep to inhibit the activities of HDACs and EZH2, respectively. Interestingly, we found TSA induced a biphasic transcriptional response: at low concentrations TSA enhanced PSA and FKBP5 transcript levels but at high concentrations it was repressive, suggesting a possible dual (activation and repression) function for HDACs in maintaining AR transcriptional activity (Figure 6B). As for DZNep, it enhanced the expression of both PSA and FKBP5, indicating a role for EZH2 in suppressing AR transcriptional activity (Figure 6C).

Besides VCaP cells, we also examined the effects of HDACs and EZH2 on AR-dependent transcription in LNCaP cells (an AR-positive but ERG negative prostate cancer cell line). Interestingly, HDACs and EZH2 were recruited to ARBS in LNCaP cells but this was in most instances lower (with respect to % input) than VCaP cells (Supplementary Figure S5). In addition, when we treated the LNCaP cells with DZNep or TSA, there was a much weaker or no response in androgen upregulation of model AR target genes, respectively (Supplementary Figure S6). Our results therefore suggest that the suppression of AR activity by HDACs and EZH2 might be more pronounced in an ERG-fusion positive prostate cancer system such as VCaP cells, however, additional experiments

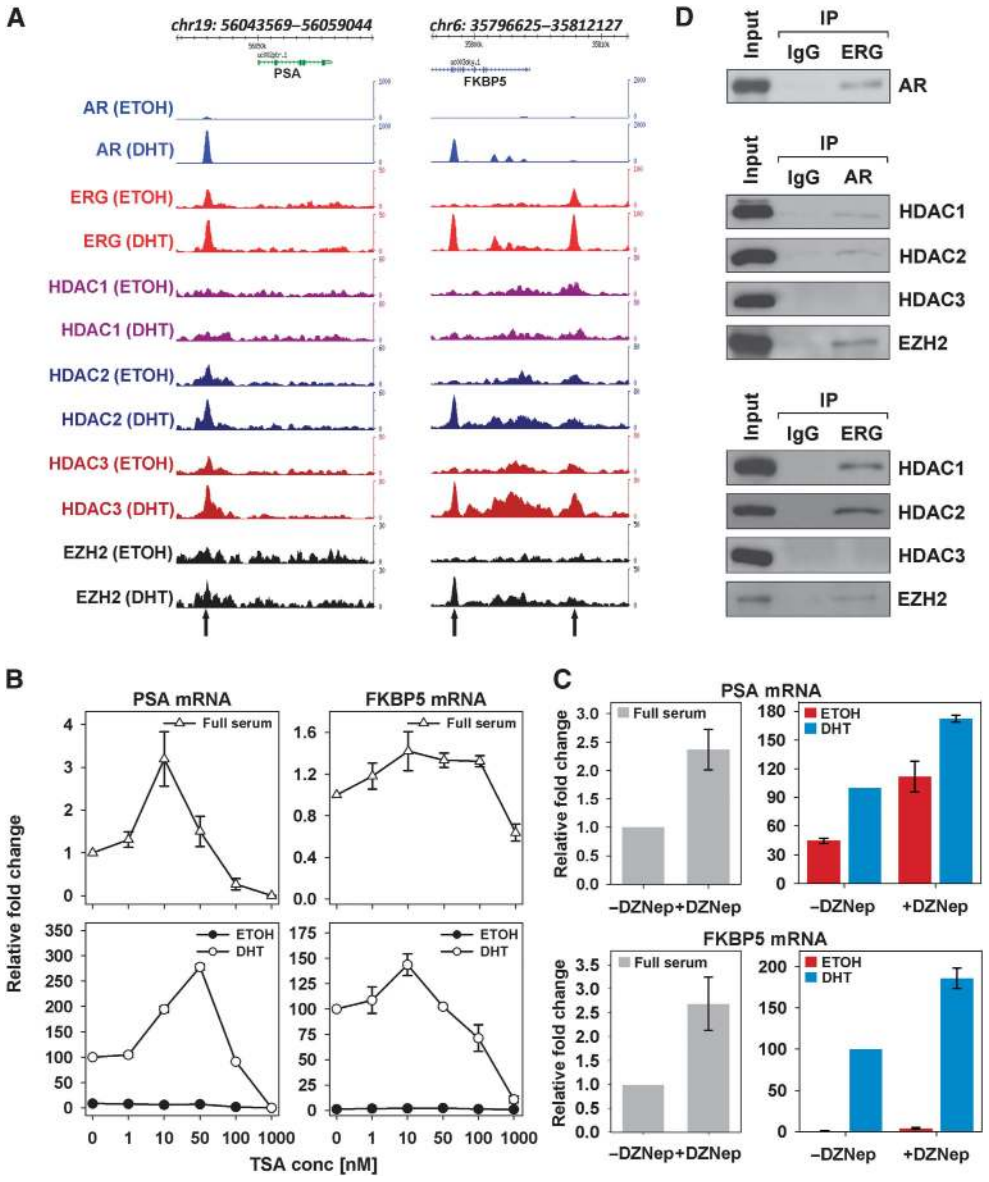

Figure 6 Co-recruitment of ERG, HDACs, and EZH2 to ARBS attenuates AR-dependent transcription. (**A**) Snapshots showing the localization of HDAC1, HDAC2, HDAC3, and EZH2 with AR and ERG at model AR target genes, PSA and FKBP5. (**B**) VCaP cells grown in full serum (top) or depleted with hormones and co-treated with vehicle/10 nM DHT for 24 h (bottom) were subjected to varying concentrations of TSA for 24 h. Total RNA from the treated cells were then harvested and converted to cDNA before quantifying for gene expression levels by qPCR. GAPDH was used as an internal normalization control. Error bars represent s.e.m. of at least 3 independent experiments. (**C**) VCaP cells grown in full serum (left) or depleted with hormone and treated with vehicle/10 nM DHT for 8 h (right) were first subjected to vehicle/3 μM DZNep treatment for 24 (left) or 48 (right) h. Total RNA was extracted and processed as described in Figure 6B. Error bars represent s.e.m. of at least 3 independent experiments. (**D**) Western blot analysis showing the endogenous interactions between AR and ERG with HDAC1, HDAC2, HDAC3, and EZH2 in VCaP cells.

will be required to determine the nature of the corepressor complex in the absence of ERG in future studies.

The recruitment of HDACs and EZH2 at AR and ERG co-localized binding sites also suggests these factors may physically interact with each other to function together. To examine this, we performed co-immunoprecipitation experiments with AR, ERG and the corepressors. Although, we had difficulty detecting interactions between HDAC3 with either AR or ERG, we were however able to observe interactions between HDAC1, HDAC2 and EZH2 with both AR and ERG (Figure 6D). Taken together, our results suggest HDACs and EZH2 may function together with AR and ERG to regulate androgen-dependent transcription.

ERG, HDACs and EZH2 mediate prostate cancer progression by inhibiting the AR-dependent transcription of Vinculin

Recent studies suggest that ERG inhibits dedifferentiation, expedites EMT and promotes metastasis in prostate cancer cells by directly activating the expression of genes such as PLA1A, PLAT, PLAU, and EZH2 (Tomlins *et al*, 2008; Yu *et al*, 2010b). The findings from this study indicate that ERG may also function as a repressor of AR-dependent transcription by working together with corepressors including HDACs and EZH2. However, whether ERG can facilitate prostate cancer progression through other mechanisms or pathways such as directly suppressing AR-mediated differentiation is unclear.

To examine if ERG inhibition of AR-dependent transcription is required for prostate cancer development, we performed a molecular concept map (MCM) analysis with androgen-upregulated genes that are associated with ERGBS. As shown in Figure 7A and in Supplementary Table S4, we found ERG bound androgen induced genes were enriched in several concepts related to prostate cancer, in particular with those that are over-expressed in cancer but repressed in advanced and metastatic prostate cancer. We also performed additional analysis on a more extensive clinical prostate cancer dataset (Taylor *et al*, 2010) and observed similar findings (Supplementary Figure S7). Specifically, the same androgen upregulated gene signature was found to be expressed significantly higher in primary prostate tumors (compared to normal prostate) but lower in metastatic prostate tumors (compared to primary tumors).

When we examined in detail the androgen regulated genes that were associated with ERGBS, we were able to identify previously reported mediators of mesenchymal epithelial transition (MET) in breast cancer including KRT8 and KRT18 (Buhler and Schaller, 2005; Tomaskovic-Crook *et al*, 2009) (Supplementary Figure S8). We confirmed by RT–qPCR the expression of these keratin genes are indeed upregulated in VCaP cells upon androgen stimulation and enhanced after ERG silencing (Supplementary Figure S8). Besides keratin genes, one potential AR target gene that we speculated ERG might suppress to facilitate metastasis in prostate cancer was Vinculin (VCL). VCL is a membrane cytoskeletal protein that is required for regulating focal adhesion turnover, a process that is important for proper cell movement (Saunders *et al*, 2006). Moreover, VCL was recently shown to interact with the MET mediator, E-Cadherin, to enhance mechanosensing (le Duc *et al*, 2010). From clinical data in the Oncomine database, we found the mRNA expression of VCL was low in primary prostate cancers and even lower in advanced metastatic counterparts (Figure 7B and Supplementary Figure S9). In addition, there was a negative correlation relationship between the mRNA levels of ERG and VCL, supporting our observations that ERG inhibits the androgen up-regulation of VCL expression (Figure 7C and Supplementary Figure S9). Finally, survival analysis using data from the Taylor *et al* clinical study (Taylor *et al*, 2010) showed patients with low expression of VCL have a significantly lower recurrence free survival (Figure 7D).

To determine whether inhibition of VCL directly links ERG and AR with prostate cancer progression, we first confirmed VCL is a direct target of AR and ERG. As shown in Figure 7E, AR and ERG are recruited to an intronic region of VCL. Moreover, siRNA mediated silencing of ERG enhanced VCL expression (Figure 7F). From our binding and small molecule inhibitor studies, we showed ERG most likely also inhibits VCL together with HDACs and EZH2 (Figure 7G–H). Finally, to assess if VCL inhibits prostate cancer metastasis we performed invasion assays with VCaP cells treated with or without siRNA against VCL. Our results showed that silencing of VCL (Figure 7I) increased the matrigel invasiveness of VCaP cells (Figure 7J and Supplementary Figure S10), and this was not due to differences in either cell death (Figure 7K) or cell proliferation (Figure 7L). Similar results were also observed in LNCaP cells (Supplementary Figure S11). Overall, our results suggest ERG promotes prostate cancer cell invasion by suppressing the AR-dependent upregulation of VCL.

Discussion

AR-mediated transcription is a complex multi-step process involving the coordinated recruitment of the receptor, collaborative factors, coactivators, and corepressors in a precise temporal and spatial manner. While most studies to date have focused on the role of coactivators such as SRCs and p300 in the activation of AR-dependent transcription, our understanding of how corepressors attenuate AR transcriptional activity and the functional consequences downstream of this regulation in prostate cancer, especially at the genomic level, is currently unclear. In this study, we used chromatin immunoprecipitation coupled to massively parallel sequencing (ChIP-Seq) to map the genome-wide binding profiles of AR and ERG, as well as commonly over-expressed transcriptional corepressors including HDAC1, HDAC2, HDAC3, and EZH2 in prostate cancer cells before and after androgen stimulation. Our results revealed ERG, HDACs and EZH2 are integrated into an AR transcriptional network that is required for the direct suppression of AR-dependent transcription. Moreover, we showed this AR transcription program includes genes that promote epithelial differentiation and inhibition of metastasis. Overall, our work implicates HDACs and the polycomb protein, EZH2 as novel oncogenic corepressors of

Figure 7 ERG, HDACs, and EZH2 promote cell invasiveness and inhibit epithelial differentiation by antagonizing AR-dependent transcription of cytoskeletal genes. (**A**) A network showing prostate cancer clinical gene signatures that are related to ERG-associated androgen upregulated genes. Oncomine Molecular Concept Map analysis was performed to compare ERG-associated (5 kb from TSS) androgen induced genes (>2 fold) that were identified in our study against clinical prostate cancer gene signatures available in the Oncomine database. The criteria for significant associations between node is defined as OD $>=2$; *P*-value $<$ 1e-4. (**B**) Boxplot showing the relative mRNA expression of VCL in clinical prostate samples from the Yu *et al* (2004) study, which has been deposited in the Oncomine database. (**C**) Scatterplot showing the relative mRNA expression of VCL and its corresponding ERG mRNA expression in clinical prostate samples from the Yu *et al* (2004) study. (**D**) Kaplan-Meier survival curve (using data from the MSKCC dataset) showing the differences in the risk of biochemical relapse between prostate cancer patients expressing high (red line) or low (green line) VCL levels. (**E**) Snapshot showing the localization of AR, ERG, HDAC1, HDAC2, HDAC3, and EZH2 at the regulatory region of VCL. (**F**) The effect of AR and ERG silencing on VCL gene expression was analyzed as described in Figure 3D, E. Error bars represent s.e.m. of at least 3 independent experiments. (**G**) The effect of TSA on the androgen-dependent gene regulation of VCL was analyzed as described in Figure 6B. Error bars represent s.e.m. of at least 3 independent experiments. (**H**) The effect of DZNep on the androgen-dependent gene regulation of VCL was analyzed as described in Figure 6C. Error bars represent s.e.m. of at least 3 independent experiments. (**I**) Western blot analysis showing VCL expression in VCaP cells growing in normal full serum media treated with control siRNA or siRNA against VCL. GAPDH was used as a loading control. (**J**) VCaP cells transfected with control siRNA or siRNA targeting VCL were subjected to Matrigel invasion assay. The number of cells per high power field (HPF) that passed through the transwell was counted. Error bars represent s.e.m. of at least 3 independent experiments. (**K**) The effect of VCL suppression on cancer cell survival was assessed by flow cytometry. siRNA transfected cells were fixed prior staining with propidium iodide for flow analysis. Analysis was presented as % of total number of gated cells in the subG1 phase. (**L**) The effect of VCL suppression on cancer cell proliferation was assessed by flow cytometry. siRNA transfected cells were incubated with BrdU for 48 h prior to fixing. The fixed cells were then stained with BrdU antibodies and 7-AAD before flow cytometry analysis was performed. Analysis was presented as % of total number of gated cells in the S phase of the cell cycle.

androgen signalling, impeding epithelial differentiation and contributing to prostate cancer progression, in part through modulating the transcriptional output of AR and ERG.

TMPRSS2:ERG is the most common form of ETS gene fusion found in prostate cancers (Kumar-Sinha *et al*, 2008). Previous studies showed that ERG can bind to the enhancer ARBS of the androgen-regulated gene, PSA, suggesting a potential collaboration between AR and ERG (Sun *et al*, 2008). From our global analysis of these two factors, we found there is a widespread co-localization of AR and ERG after 2 h of DHT stimulation (Figure 2), which indicates the collaboration between these two factors occurs throughout the prostate cancer genome. During the course of this work, a genome-wide map of AR and ERG, also in VCaP cells, was reported (Yu *et al*, 2010b). Although the experimental conditions were different, the cistromic maps generated in both studies overlap well with each other (Supplementary Figure S12). In contrast to the other study, which only examined AR binding after a long period of androgen stimulation and ERG binding only under full serum condition, our study here provides an extensive profile of AR and ERG binding before and after androgen stimulation at short and

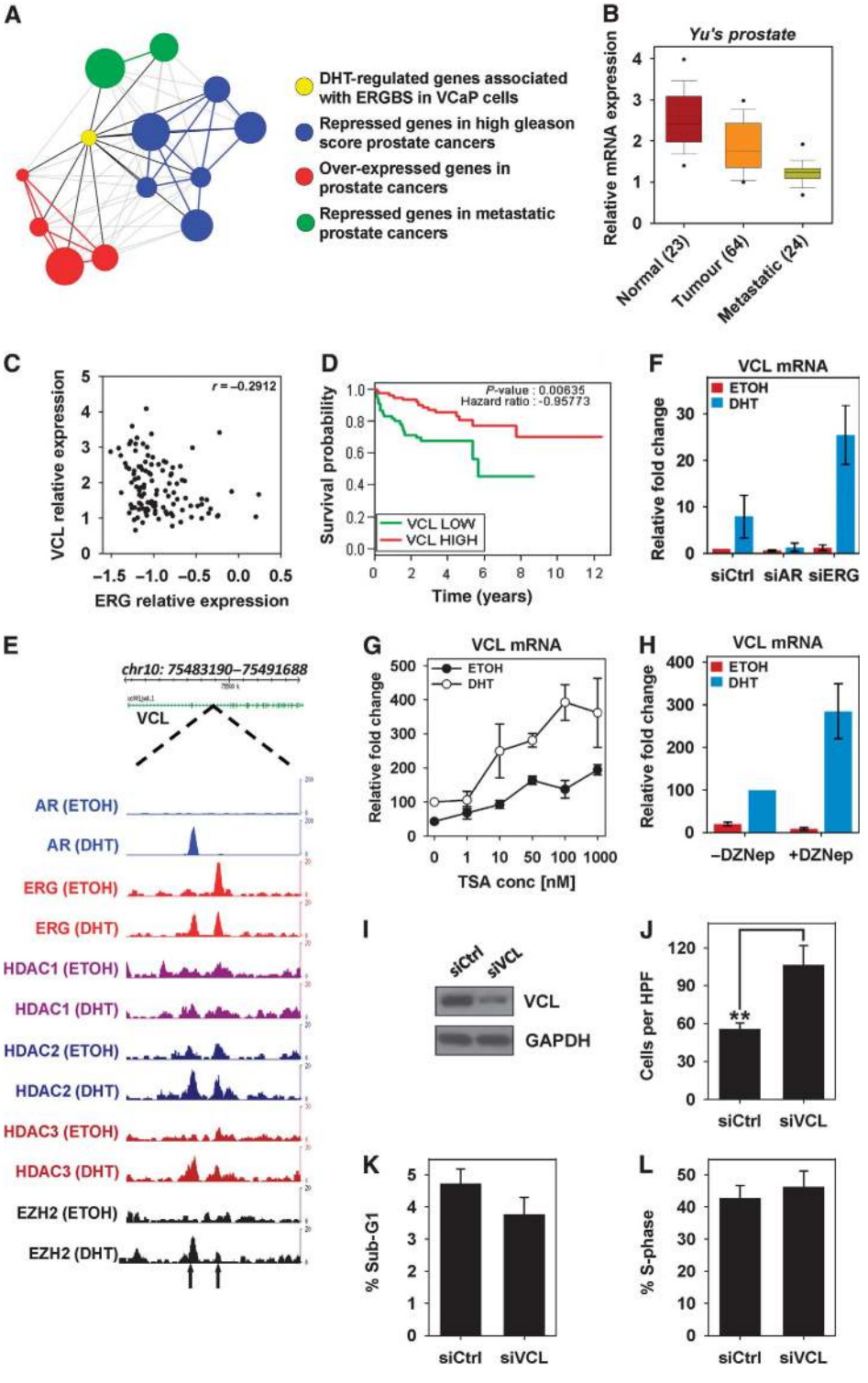

long time intervals. From our time-course ChIP-Seq of AR and ERG, we uncovered several surprising insights into the mechanism of AR- and ERG-mediated transcriptional regulation during androgen signalling. Specifically, our study revealed that ERG in general was pre-bound to chromatin at ERG unique and AR + ERG co-localized binding sites prior to androgen stimulation (Figure 2). This finding was unexpected since the expression of ERG is thought to be androgen-regulated due to a fusion event (Tomlins *et al*, 2005). However, as shown in our western blot analysis of ERG (Figure 1B), there is already a significant level of the protein expressed in VCaP cells before androgen stimulation, which likely explains why ERG can bind to chromatin before androgen stimulation. Although ERG is pre-bound to chromatin, our time-course ChIP-Seq showed that the recruitment of ERG to AR + ERG co-localized binding sites can be further enhanced with short-term DHT stimulation, while the increment of ERG at ERG unique sites occurred mainly after a rise in ERG levels stemming from prolonged androgen stimulation (Figure 2). This observation suggests that additional ERG recruitment to ARBS may be enhanced by AR binding. Moreover, this result shows that ERG is unlike other transcriptional repressors of nuclear receptors such as NKX3-1 and LEF-1, which compete with the Estrogen Receptor (ER) for binding to the ER binding sites (Holmes *et al*, 2008). Finally, we also noticed from our ChIP-Seq study that apart from being recruited at AR-bound enhancers, ERG was frequently located at the promoters of AR target genes as well (Supplementary Figure S13). This binding was usually independent of AR recruitment. Whether ERG binding at the promoter region is required for the repression of AR target genes will require further studies in the future.

Besides AR and ERG, numerous transcriptional corepressors are also frequently over-expressed in prostate cancers (Varambally *et al*, 2002; Weichert *et al*, 2008). Through genome-wide binding analysis, we discovered the existence of a closely knitted and intricate transcriptional network between AR and ERG, as well as the frequently over-expressed corepressor proteins, HDAC1, HDAC2, HDAC3, and EZH2. Strikingly, this transcriptional network is highly regulated by and responsive to androgen stimulation (Figure 5). In general, our study showed that androgen signalling culminates in an increased occupancy of AR, ERG, HDAC2, HDAC3, and EZH2 to shared elements in the network (Figure 5). Although HDACs have been shown to play a role in nuclear receptor transcription (Shang *et al*, 2002; Burd *et al*, 2006), our finding that EZH2 is co-localized at ARBS was rather surprising since EZH2 is mainly associated with the methylation of histones at the promoter of repressed genes (Yu *et al*, 2007a; Ku *et al*, 2008; Margueron *et al*, 2008). Even though our results suggest that ERG can engage HDACs and EZH2 (Figures 5 and 6) to suppress androgen signalling in ERG-positive VCaP prostate cancer cells, the specificity and mechanism of their transcriptional co-operation are still not completely clear and will therefore require further detailed analysis.

Since TMPRSS2:ERG is a recurrent gene fusion widely expressed in prostate cancers, it was not surprising to find that it has important roles in prostate cancer initiation and progression (Zong *et al*, 2009). Although our work and others (Sun *et al*, 2008; Yu *et al*, 2010b) showed that ERG repressed AR-mediated induction of differentiation markers such as PSA and FKBP5, these markers have no major known functional role in prostate cancer differentiation and progression (Chen and Sawyers, 2010). However, from our gene association analysis, we found that ERG-associated androgen induced genes are highly associated with metastatic prostate cancers and thus might be involved in cellular processes such as Epithelial Mesenchymal Transition (EMT) that promote cell invasion.

In the EMT process, epithelial markers including keratins and E-Cadherins will be replaced with mesenchymal markers such as Vimentin and N-Cadherins (Lee *et al*, 2006). This change in the composition of the cell adhesion and cytoskeleton molecules will inevitably lead to a decrease in cell adhesion as well as cell-cell cohesion and in turn, culminate into an increase in cell invasiveness (Lee *et al*, 2006). Interestingly, from our work we noticed several epithelial keratin proteins (e.g. KRT8 and KRT18) that were upregulated by androgen stimulation (Supplementary Figure S8). Thus, our findings suggest that by repressing the expression of epithelial cell adhesion and cytoskeletal molecules through inhibition of AR signalling, ERG could potentially promote EMT and confer metastatic properties. Indeed, we identified the AR-induced but ERG repressed gene, VCL, as a novel suppressor of prostate cancer cell invasiveness. Interestingly, VCL was recently shown to potentiate E-cadherin mechanosensing (le Duc *et al*, 2010) and therefore may be required for the optimal function of E-cadherin.

Given that androgen is the main driver of prostate cancer progression, it was contradicting that studies showed high doses of DHT treatment could slow prostate cancer progression (Tsihlias *et al*, 2000; Hofman *et al*, 2001). This phenomenon could be partially explained by the dual opposing role of AR in prostate cancer progression. On one hand, AR can promote proliferation and inhibits apoptosis. On the other hand, AR can also halt cancer progression and metastasis by inducing differentiation and enhancing an epithelial phenotype. Moreover, a recent study by Zhu and Kyprianou (Zhu and Kyprianou, 2010) showed that a low AR content is required for an EMT phenotype in prostate cancers. These findings suggest that AR signalling requires fine-tuning to an optimal level in order to favor prostate cancer progression. Our study is in agreement with these observations and provides a molecular explanation for how AR can regulate these two distinct processes in prostate cancer. Taken together, our findings show that a highly integrated transcriptional network of AR and ERG, together with HDACs and EZH2, exists to advance the development of prostate cancers to a metastable state by restraining epithelial differentiation and promoting EMT through regulated suppression of AR signalling.

Materials and methods

Cell culture

The human prostate cancer cell lines, LNCaP and VCaP were obtained from American Type Culture Collection. VCaP cells were maintained in DMEM supplemented with 10% fetal bovine serum (FBS), sodium pyruvate, sodium bicarbonate, and penicillin/streptomycin at 37°C under 5% CO_2. LNCaP cells were maintained in RPMI medium 1640 supplemented with 10% FBS, sodium pyruvate, gentamycin and penicillin/streptomycin at 37°C under 5% CO_2. Unless otherwise stated, for experiments requiring DHT (Tokyo Chemical Industry) treatment, VCaP cells were grown for 24 h prior to stimulation in phenol red free DMEM supplemented with 10% charcoal-dextran stripped fetal bovine serum (CDFBS), sodium pyruvate, sodium bicarbonate, and penicillin/streptomycin, while LNCaP cells were grown for 72 h prior to stimulation in phenol red

free RPMI supplemented with 5% CDFBS, sodium pyruvate, gentamycin, and penicillin/streptomycin.

Gene expression analysis

Cells were harvested and total RNA was collected in TRI-reagent (Sigma) and purified with PureLink™ RNA Mini Kit (Invitrogen). Reverse transcription of RNA to cDNA was carried out using M-MLV reverse transcriptase (Promega). RNA expression levels were measured using quantitative PCR and normalized to GAPDH. The primers for cDNA quantification can be found in Supplementary Table S5.

Microarray expression profiling

Purified total RNA from three independent biological replicates of VCaP cells exposed to varying lengths of DHT stimulation were converted to cRNA using the Illumina® TotalPrepTM-96 RNA Amplification Kit (Ambion) according to the manufacturer's instructions. cRNA was hybridized onto Sentrix® HumanRef-8 v3 Expression BeadChip Kit (Illumina). The BeadChips were scanned with the BeadArray Reader and the image data was processed using GenomeStudio. The gene expression data was analyzed using GeneSpring GX 11.0 software.

Western blot analysis

The antibodies used for western blot analysis include anti-AR (sc-816), anti-ERG (sc-354), anti-Vinculin (sc-25336) from Santa Cruz, anti-AR (AR441) from Labvision, anti-HDAC1 (#05-100), anti-HDAC2 (#05-814) from Millipore, anti-HDAC3 (#3949) and anti-EZH2 (#3147) from Cell signalling Technology.

Chromatin immunoprecipitation (ChIP)

ChIP assay was performed as described previously (Tan *et al*, 2011). All ChIP-qPCR primer sequences can be found in Supplementary Table S6 and S7. For HDAC1, HDAC2, HDAC3, and EZH2 ChIP, a double cross-linking strategy was used to stabilize protein-protein interactions. Specifically, cells were first fixed with 2 mM DSG (Pierce) for 45 min prior to formaldehyde fixation. Antibodies that were used for ChIP analysis include anti-AR (sc-815x), anti-ERG (sc-353), anti-HDAC3 (sc-11417) from Santa Cruz Biotechnology, anti-HDAC1 (ab7028-50), anti-HDAC2 (ab7029-50) from Abcam, and anti-EZH2 (39639/39901) from Active Motif. The specificity of the antibodies used for ChIP assays were validated in western blot assays with VCaP cells that were treated with siRNAs targeting the different specific transcription factor (Supplementary Figure S14).

Co-immunoprecipitation

All co-IP experiments were performed with VCaP cells grown in full serum conditions. VCaP cells were trypsinized and lysed to obtain whole cell lysate. The cell lysate was subsequently pre-cleared with Protein A/G-Agarose beads (Roche Applied Science) at 4°C for 4 h. An aliquot of the whole cell lysate was collected and stored at -80°C as input for the western blot analysis. After pre-clearing, the supernatant was incubated overnight at 4°C with 5 μg of anti-AR (sc-815x) or anti-ERG (sc-353). Roche beads were added into the mixture on the next day and incubated for 1.5 h at 4°C, and then washed with TBS for four times. Finally, the beads were heated to 99°C for 5 min and eluted with SDS loading buffer for western blot analysis.

Short interfering RNAs (siRNAs)

Unless otherwise stated, siRNA studies were carried out using a double knockdown approach. Briefly, VCaP cells were transfected twice with the selected siRNA at a concentration of 100 nM/transfection using Lipofectamine RNAi Max (Invitrogen) with a 24 h interval between each transfection. The siRNAs used in this study were siAR (ON-TARGETplus SMARTpool L-003400-00), siERG (SiGENOME D-003886-01), siHDAC1 (ON-TARGETplus SMARTpool L-003493-00), siHDAC2 (ON-TARGETplus SMARTpool L-003495-00), siHDAC3 (ON-TARGETplus SMARTpool L-003496-00), siEZH2 (ON-TARGETplus SMARTpool L-004218-00) from Dharmacon, and siVCL synthesized from 1stBase. The siVCL sequence is rCrUrGrGrCrUrUrGrCrArGrArUrCrCrArArArUrUrU. The control siRNA for the siAR, siERG, siHDAC1/2/3 and siEZH2 experiments was from Dharmacon (D-001206-13), while the control siRNA for the siVCL experiments was from 1stBase (rUrUrCrUrCrCrGrArArCrGrUrGrUrCrArCrGrUTT).

ChIP-Seq

ChIP-Seq was performed as described previously (Tan *et al*, 2011). ChIP-Seq reads were aligned to the reference human genome (UCSC, hg18) and binding peaks using input reads as control were determined with CCAT (Xu *et al*, 2010).

Matrigel invasion assay

Invasion assay was performed using (8.0 μm pore size) HTS FluoroBlok Cell Culture Inserts (BD). Briefly, 750 μl of media (with 20% FBS) was added into each well of a 24-well plate and inserts were placed individually into each well. Each insert was first coated with 80 μl of the pre-diluted (250 μg/ml) Matrigel Basement Matrix (BD). Next, 4×10^5 siRNA-treated VCaP cells/2×10^5 siRNA-treated LNCaP cells in 200 μl media (with 0.5% FBS) were seeded into each well. After 48 h, the cells at the bottom of the inserts were fixed with 3.7% formaldehyde for 15–30 min prior to staining with 25 μg/ml propidium iodide for 30–60 min in the dark. Any cells that passed through the base membrane of the inserts were then scanned by a Cellomics Arrayscan. Ten different fields were taken for each insert. Each condition was assayed in technical triplicates for biological triplicates.

Conservation analysis for binding peaks

Conservation scores for the alignment of 27 vertebrate genomes with Human (PhastCons28way) were downloaded from the UCSC Genome Browser database. The sequence conservation score for every position in a 2000 bp window centering on the defined ChIP-Seq peak/cluster were plotted for comparison.

Generation of heatmap binding signals

ERG and AR binding peaks that were within 500 bp of each other were clustered together for the generation of the plot. For a fair comparison of tag intensity, the AR and ERG libraries were re-sampled to 10 million reads before being plotted out as binding signals around a region of $-/+2$ kb centralized at the respective AR/ERG ChIP-Seq peak or defined AR/ERG clusters ($-/+2$ kb). The individual binding region was sorted by their binding signals at their respective categories (AR only, ERG only and AR/ERG overlap) for easy visualization.

Data deposition

Raw ChIP-Seq and gene expression profiling data generated from this study have been deposited at the NCBI GEO repository under accession number GSE28951.

Supplementary data

Supplementary data are available at *The EMBO Journal* Online (http://www.embojournal.org).

Acknowledgements

We would like to thank the GTB and the IT groups at GIS for sequencing support and Peiyong Guan for advice on survival analysis. We would also like to thank Dr Yu Qiang for generously providing TSA and DZNep. This work was supported by the Biomedical Research Council/Science and Engineering Research Council of A*STAR (Agency for Science and Technology), Singapore. KRC and CWC are supported by A*STAR graduate scholarships. SKT and YC are supported by a NUS Graduate School for Integrative Sciences and Engineering Scholarship.

Author contributions: KRC designed and performed most of the experiments. SKT performed the microarray experiments. CY validated the ChIP-Seq data and performed the interactions studies. SZH performed the inhibitor studies. NYWS performed the western blot analyses. CWC carried out all the bioinformatic analyses. EC conceived and supervised the study. KRC and EC analyzed the data and wrote the manuscript.

Conflict of interest

The authors declare that they have no conflict of interest.

References

Bjorkman M, Iljin K, Halonen P, Sara H, Kaivanto E, Nees M, Kallioniemi OP (2008) Defining the molecular action of HDAC inhibitors and synergism with androgen deprivation in ERG-positive prostate cancer. *Int J Cancer* **123:** 2774–2781

Buhler H, Schaller G (2005) Transfection of keratin 18 gene in human breast cancer cells causes induction of adhesion proteins and dramatic regression of malignancy *in vitro* and *in vivo*. *Mol Cancer Res* **3:** 365–371

Burd CJ, Morey LM, Knudsen KE (2006) Androgen receptor corepressors and prostate cancer. *Endocr Relat Cancer* **13:** 979–994

Cao Q, Yu J, Dhanasekaran SM, Kim JH, Mani RS, Tomlins SA, Mehra R, Laxman B, Cao X, Kleer CG, Varambally S, Chinnaiyan AM (2008) Repression of E-cadherin by the polycomb group protein EZH2 in cancer. *Oncogene* **27:** 7274–7284

Cao R, Zhang Y (2004) The functions of E(Z)/EZH2-mediated methylation of lysine 27 in histone H3. *Curr Opin Genet Dev* **14:** 155–164

Chen Y, Sawyers CL (2010) Coordinate transcriptional regulation by ERG and androgen receptor in fusion-positive prostate cancers. *Cancer Cell* **17:** 415–416

Glozak MA, Seto E (2007) Histone deacetylases and cancer. *Oncogene* **26:** 5420–5432

Gupta S, Iljin K, Sara H, Mpindi JP, Mirtti T, Vainio P, Rantala J, Alanen K, Nees M, Kallioniemi O (2010) FZD4 as a mediator of ERG oncogene-induced WNT signaling and epithelial-to-mesenchymal transition in human prostate cancer cells. *Cancer Res* **70:** 6735–6745

Heinlein CA, Chang C (2004) Androgen receptor in prostate cancer. *Endocrine Rev* **25:** 276–308

Hofman K, Swinnen JV, Verhoeven G, Heyns W (2001) E2F activity is biphasically regulated by androgens in LNCaP cells. *Biochem Biophys Res Commun* **283:** 97–101

Holmes KA, Song JS, Liu XS, Brown M, Carroll JS (2008) Nkx3-1 and LEF-1 function as transcriptional inhibitors of estrogen receptor activity. *Cancer Res* **68:** 7380–7385

Iljin K, Wolf M, Edgren H, Gupta S, Kilpinen S, Skotheim RI, Peltola M, Smit F, Verhaegh G, Schalken J, Nees M, Kallioniemi O (2006) TMPRSS2 fusions with oncogenic ETS factors in prostate cancer involve unbalanced genomic rearrangements and are associated with HDAC1 and epigenetic reprogramming. *Cancer Res* **66:** 10242–10246

Ku M, Koche RP, Rheinbay E, Mendenhall EM, Endoh M, Mikkelsen TS, Presser A, Nusbaum C, Xie X, Chi AS, Adli M, Kasif S, Ptaszek LM, Cowan CA, Lander ES, Koseki H, Bernstein BE (2008) Genomewide analysis of PRC1 and PRC2 occupancy identifies two classes of bivalent domains. *PLoS Genet* **4:** e1000242

Kumar-Sinha C, Tomlins SA, Chinnaiyan AM (2008) Recurrent gene fusions in prostate cancer. *Nat Rev Cancer* **8:** 497–511

le Duc Q, Shi Q, Blonk I, Sonnenberg A, Wang N, Leckband D, de Rooij J (2010) Vinculin potentiates E-cadherin mechanosensing and is recruited to actin-anchored sites within adherens junctions in a myosin II-dependent manner. *J Cell Biol* **189:** 1107–1115

Lee JM, Dedhar S, Kalluri R, Thompson EW (2006) The epithelial-mesenchymal transition: new insights in signaling, development, and disease. *J Cell Biol 172*973–981

Lee ST, Li Z, Wu Z, Aau M, Guan P, Karuturi RK, Liou YC, Yu Q (2011) Context-specific regulation of NF-kappaB target gene expression by EZH2 in breast cancers. *Mol Cell* **43:** 798–810

Margueron R, Li G, Sarma K, Blais A, Zavadil J, Woodcock CL, Dynlacht BD, Reinberg D (2008) Ezh1 and Ezh2 maintain repressive chromatin through different mechanisms. *Mol Cell* **32:** 503–518

Massie CE, Adryan B, Barbosa-Morais NL, Lynch AG, Tran MG, Neal DE, Mills IG (2007) New androgen receptor genomic targets show an interaction with the ETS1 transcription factor. *EMBO Rep* **8:** 871–878

Min J, Zaslavsky A, Fedele G, McLaughlin SK, Reczek EE, De Raedt T, Guney I, Strochlic DE, Macconaill LE, Beroukhim R, Bronson RT, Ryeom S, Hahn WC, Loda M, Cichowski K (2010) An oncogene-tumor suppressor cascade drives metastatic prostate cancer by coordinately activating Ras and nuclear factor-kappaB. *Nat Med* **16:** 286–294

Pienta KJ, Bradley D (2006) Mechanisms underlying the development of androgen-independent prostate cancer. *Clin Cancer Res* **12:** 1665–1671

Saunders RM, Holt MR, Jennings L, Sutton DH, Barsukov IL, Bobkov A, Liddington RC, Adamson EA, Dunn GA, Critchley DR (2006) Role of vinculin in regulating focal adhesion turnover. *Eur J Cell Biol* **85:** 487–500

Schiewer MJ, Augello MA, Knudsen KE (2012) The AR dependent cell cycle: mechanisms and cancer relevance. *Mol Cell Endocrinol* **352:** 34–45

Shang Y, Myers M, Brown M (2002) Formation of the androgen receptor transcription complex. *Mol Cell* **9:** 601–610

Shen MM, Abate-Shen C (2010) Molecular genetics of prostate cancer: new prospects for old challenges. *Genes Dev* **24:** 1967–2000

Shin S, Kim TD, Jin F, van Deursen JM, Dehm SM, Tindall DJ, Grande JP, Munz JM, Vasmatzis G, Janknecht R (2009) Induction of prostatic intraepithelial neoplasia and modulation of androgen receptor by ETS variant 1/ETS-related protein 81. *Cancer Res* **69:** 8102–8110

Sun C, Dobi A, Mohamed A, Li H, Thangapazham RL, Furusato B, Shaheduzzaman S, Tan SH, Vaidyanathan G, Whitman E, Hawksworth DJ, Chen Y, Nau M, Patel V, Vahey M, Gutkind JS, Sreenath T, Petrovics G, Sesterhenn IA, McLeod DG *et al* (2008) TMPRSS2-ERG fusion, a common genomic alteration in prostate cancer activates C-MYC and abrogates prostate epithelial differentiation. *Oncogene* **27:** 5348–5353

Tan SK, Lin ZH, Chang CW, Varang V, Chng KR, Pan YF, Yong EL, Sung WK, Cheung E (2011) AP-2gamma regulates oestrogen receptor-mediated long-range chromatin interaction and gene transcription. *EMBO J* **30:** 2569–2581

Taylor BS, Schultz N, Hieronymus H, Gopalan A, Xiao Y, Carver BS, Arora VK, Kaushik P, Cerami E, Reva B, Antipin Y, Mitsiades N, Landers T, Dolgalev I, Major JE, Wilson M, Socci ND, Lash AE, Heguy A, Eastham JA *et al* (2010) Integrative genomic profiling of human prostate cancer. *Cancer Cell* **18:** 11–22

Tomaskovic-Crook E, Thompson EW, Thiery JP (2009) Epithelial to mesenchymal transition and breast cancer. *Breast Cancer Res* **11:** 213

Tomlins SA, Laxman B, Varambally S, Cao X, Yu J, Helgeson BE, Cao Q, Prensner JR, Rubin MA, Shah RB, Mehra R, Chinnaiyan AM (2008) Role of the TMPRSS2-ERG gene fusion in prostate cancer. *Neoplasia (New York, NY)* **10:** 177–188

Tomlins SA, Rhodes DR, Perner S, Dhanasekaran SM, Mehra R, Sun X-W, Varambally S, Cao X, Tchinda J, Kuefer R, Lee C, Montie JE, Shah RB, Pienta KJ, Rubin MA, Chinnaiyan AM (2005) Recurrent fusion of TMPRSS2 and ETS transcription factor genes in prostate cancer. *Science (New York, NY)* **310:** 644–648

Tsihlias J, Zhang W, Bhattacharya N, Flanagan M, Klotz L, Slingerland J (2000) Involvement of p27Kip1 in G1 arrest by high dose 5 alpha-dihydrotestosterone in LNCaP human prostate cancer cells. *Oncogene* **19:** 670–679

Varambally S, Dhanasekaran SM, Zhou M, Barrette TR, Kumar-Sinha C, Sanda MG, Ghosh D, Pienta KJ, Sewalt RG, Otte AP, Rubin MA, Chinnaiyan AM (2002) The polycomb group protein EZH2 is involved in progression of prostate cancer. *Nature* **419:** 624–629

Wang L, Zou X, Berger AD, Twiss C, Peng Y, Li Y, Chiu J, Guo H, Satagopan J, Wilton A, Gerald W, Basch R, Wang Z, Osman I, Lee P (2009) Increased expression of histone deacetylaces (HDACs) and inhibition of prostate cancer growth and invasion by HDAC inhibitor SAHA. *Am J Transl Res* **1:** 62–71

Wang Q, Li W, Liu XS, Carroll JS, Jänne OA, Keeton EK, Chinnaiyan AM, Pienta KJ, Brown M (2007) A hierarchical network of transcription factors governs androgen receptor-dependent prostate cancer growth. *Mol Cell* **27:** 380–392

Weichert W, Roske A, Gekeler V, Beckers T, Stephan C, Jung K, Fritzsche FR, Niesporek S, Denkert C, Dietel M, Kristiansen G (2008) Histone deacetylases 1, 2 and 3 are highly expressed in prostate cancer and HDAC2 expression is associated with shorter PSA relapse time after radical prostatectomy. *Br J Cancer* **98:** 604–610

Xu H, Handoko L, Wei X, Ye C, Sheng J, Wei CL, Lin F, Sung WK (2010) A signal-noise model for significance analysis of ChIP-seq with negative control. *Bioinformatics* **26:** 1199–1204

Yu J, Cao Q, Mehra R, Laxman B, Tomlins SA, Creighton CJ, Dhanasekaran SM, Shen R, Chen G, Morris DS, Marquez VE, Shah RB, Ghosh D, Varambally S, Chinnaiyan AM (2007a)

Integrative genomics analysis reveals silencing of beta-adrenergic signaling by polycomb in prostate cancer. *Cancer Cell* **12:** 419–431

Yu J, Cao Q, Wu L, Dallol A, Li J, Chen G, Grasso C, Cao X, Lonigro RJ, Varambally S, Mehra R, Palanisamy N, Wu JY, Latif F, Chinnaiyan AM (2010a) The neuronal repellent SLIT2 is a target for repression by EZH2 in prostate cancer. *Oncogene* **29:** 5370–5380

Yu J, Rhodes DR, Tomlins SA, Cao X, Chen G, Mehra R, Wang X, Ghosh D, Shah RB, Varambally S, Pienta KJ, Chinnaiyan AM (2007b) A polycomb repression signature in metastatic prostate cancer predicts cancer outcome. *Cancer Res* **67:** 10657–10663

Yu J, Yu J, Mani R-S, Cao Q, Brenner CJ, Cao X, Wang X, Wu L, Li J, Hu M, Gong Y, Cheng H, Laxman B, Vellaichamy A, Shankar S, Li Y, Dhanasekaran SM, Morey R, Barrettezzz T, Lonigrozzz RJ *et al* (2010b) An integrated network of androgen receptor, polycomb, and TMPRSS2-ERG gene fusions in prostate cancer progression. *Cancer Cell* **17:** 443–454

Yu YP, Landsittel D, Jing L, Nelson J, Ren B, Liu L, McDonald C, Thomas R, Dhir R, Finkelstein S, Michalopoulos G, Becich M, Luo JH (2004) Gene expression alterations in prostate cancer predicting tumor aggression and preceding development of malignancy. *J Clin Oncol* **22:** 2790–2799

Zhang Z, Chang CW, Goh WL, Sung WK, Cheung E (2011) CENTDIST: discovery of co-associated factors by motif distribution. *Nucleic Acids Res* **39**(Web Server issue): W391–W399

Zhu M-L, Kyprianou N (2010) Role of androgens and the androgen receptor in epithelial-mesenchymal transition and invasion of prostate cancer cells. *FASEB J* **24:** 769–777

Zong Y, Xin L, Goldstein AS, Lawson DA, Teitell MA, Witte ON (2009) ETS family transcription factors collaborate with alternative signaling pathways to induce carcinoma from adult murine prostate cells. *Proc Natl Acad Sci USA* **106:** 12465–12470